International Journal of Advanced Robotic Systems
March-April 2019: 1–10

DOI: 10.1177/1729881419840213
journals.sagepub.com/home/arx
SAGE

An adaptive fuzzy sliding mode controller for the depth control of an underactuated underwater vehicle

Yuan Chen, Yinpo Yan, Kangling Wang and Shuqi Liu

Abstract

An adaptive fuzzy sliding mode controller is proposed for the depth control of an underactuated underwater vehicle based on the state-dependent Riccati equation. An adaptive fuzzy control algorithm is embedded into the sliding mode controller to solve the buffering and mismatched uncertain problems in the robust sliding mode variable structure controller, where an auxiliary fuzzy control unit is designed to automatically adjust the scale factor of the main fuzzy controller output. Based on Lyapunov stability theory and final value bounded theorem, the stability and convergence properties of the closed-loop system are demonstrated. Numerical simulations are carried out to validate the effectiveness of the proposed controller.

Keywords

Underactuated underwater vehicle, adaptive fuzzy sliding mode controller, depth control, state-dependent Riccati equation

Date received: 10 July 2018; accepted: 6 February 2019

Topic: Robot Manipulation and Control
Topic Editor: Andrey V Savkin
Associate Editor: Luis Tupak Aguilar Bustos

Introduction

Autonomous underwater vehicles (AUVs) have been widely used to explore ocean resources. These vehicles usually contain several critical devices to overcome hazardous underwater environment and to accomplish challenging tasks required for those vehicles. However, the effective controller of underwater vehicle continues to pose great challenges to system designers in the controller due to the system's highly nonlinear, time-varying, dynamic behaviors and uncertainties in hydrodynamic coefficients and external disturbances. The dependence of the dynamic model on the uncertain underwater environment also makes the precise control of the AUV depth more challenging. Control strategies with intelligence, adaptive capability, fast convergence, and robustness are also required.

It has already been shown[1,2] that, in the case of underwater vehicles, the traditional control methodologies are not the most suitable choice and cannot guarantee the required tracking performance. On the other hand, sliding mode control, due to its attractiveness such as robustness to parametric uncertainty, insensitivity to unknown disturbances, fast dynamic response, order reduction, easier implementation, and design simplification, has proven to be a very attractive approach to cope with these problems. However, the practical application of sliding mode controller (SMC) is limited by the lack of knowledge on the

School of Mechanical, Electrical and Information Engineering, Shandong University at Weihai, People's Republic of China

Corresponding author:
Yuan Chen, School of Mechanical, Electrical and Information Engineering, Shandong University at Weihai, 180 Wenhua Xilu, Weihai, People's Republic of China.
Email: cyzghysy@sdu.edu.cn

uncertainties of the dynamic model, including plant uncertainties and external disturbance. Many adaptive fuzzy control schemes[3–9] involving linguistic fuzzy information from human experts have been effectively integrated into SMC to circumvent the problem of uncertainties for robot. For instance, Lakhekar and Waghmare[3] developed an adaptive fuzzy proportional integral (PI) SMC for trajectory tracking control of AUV to achieve high precise maneuvering. Ma et al.[4] designed an adaptive sliding mode dynamical surface controller for a hybrid unmanned aerial underwater vehicles. Sarfraz et al.[5] presented a robust stabilizing controller via adaptive integral sliding mode for nonholonomic systems with uncertainties. Zhang et al.[6] proposed an adaptive quasi-sliding mode control method for the path following system of an underactuated unmanned underwater vehicle. Bessa et al.[7] presented an adaptive fuzzy sliding mode controller (AFSMC) for remotely operated underwater vehicles. Yang et al.[8] propose a sliding mode control law for asymptotically stabilizing a nonholonomic mobile robot to a desired trajectory. Savkin and Wang[9] presented a biologically inspired strategy for the navigation of a unicycle-like robot toward a target while avoiding collisions with moving obstacles. Although the aforementioned SMCs have been used to reduce the effects of unknown uncertainties on the control performances, those unknown uncertainties must be located exactly on the position of control output vector or in the intermediate variable in the state space equation. Such limitation on the position of the nonlinear uncertain function is usually known as the strict match condition. Unless an uncertain system satisfies the strict match condition, these aforementioned SMCs cannot be used to achieve their desired control performances for the underwater vehicle. Only few investigations[10,11] have been conducted on the design of an SMC with loosen constraints on the position of the mismatched uncertainties.

Varieties of neural networks and proportional differentials coupled with the SMC have been used to address the chattering problem in the general SMC. Chatchanayuenyong et al.[12] proposed a neural network-based time optimal SMC to determine the solution of the nonlinear curve. However, the tuning of neuron weights requires a large quantity of experimental datum. Wang et al.[13] designed an SMC that has multivariable output feedback adaptive terminal. Although the convergence of the closed loop system is achieved using Lyapunov stability theory, some tracking errors are not bounded within a small tolerance region. Ouyang et al.[14] developed a proportional differential plus SMC to compensate for the uncertainties. However, the controller is not robust enough in terms of the proportional–derivative (PD) control gain. Many fuzzy control schemes involving linguistic fuzzy information from human experts were also integrated into the SMC to circumvent the chattering problem. For instance, Chen and Zhang[15] applied an adaptive fuzzy sliding mode control algorithm to resolve the system chattering problem. Aloui et al.[16] designed an AFSMC with an adaptive PI term to minimize the chattering phenomenon. Lakhekar et al.[17] proposed two types of fuzzy approximations to cope with chattering problem. Lakhekar et al.[18] introduced two types of fuzzy self-turning techniques to eliminate the effects of chattering. Amer et al.[19] developed a reduced rule-based fuzzy proportional integral SMC to eliminate chattering. Esfahani et al.[20] designed an AFSMC to address the problems of chattering under the condition of lacking training data and non-robust tracking errors.

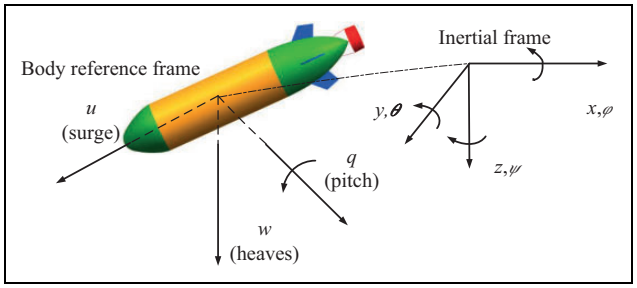

Figure 1. Schematic of REMUS underwater vehicle. REMUS: remote environmental unit.

In this article, an AFSMC is proposed for the depth control of an underactuated underwater vehicle based on the state-dependent Riccati equation. An adaptive fuzzy control algorithm is embedded into the SMC to solve the buffering and mismatched uncertain problems in the robust sliding mode variable structure controller, where an auxiliary fuzzy control unit is designed to automatically adjust the scale factor of the main fuzzy controller output. Based on Lyapunov stability theory and final value bounded theorem, the stability and convergence properties of the closed-loop system are demonstrated. Numerical simulations are carried out to validate the effectiveness of the proposed controller.

This article is organized as follows. In the second section, the nominal model and uncertainty model of an underwater vehicle are formulated. In the third section, an adaptive fuzzy robust SMC is designed along with the assessment in its convergence. In the fourth section, the numerical simulation results are presented and discussed. Conclusion is given in the fifth section.

Dynamic modeling of underwater vehicle

Modeling

The Remote Environmental Unit (REMUS) AUV[21] and its corresponding reference frames are illustrated in Figure 1. The inertial reference frame is considered a fixed frame, whose z-axis directed into the gravitational direction and the other two axes are perpendicular to the z-axis. In contrast, the body reference frame is set at the geometric center of the underwater vehicle. The longitudinal u-axis directed into the direction from the tail to the nose, and the vertical w-axis is along the direction from the top to the bottom. The

underwater vehicle is assumed a rigid body with a symmetrical longitudinal plane.

The nonlinear dynamic model of a 3-DOF underactuated underwater vehicle in the inertial frame can be written in the following uniform matrix form

$$\begin{aligned} m[\dot{w} - uq - x_G\dot{q} - z_G q^2] = {} & Z_{\dot{q}}\dot{q} + Z_{\dot{w}}\dot{w} + Z_{uq}uq + Z_{uw}uw \\ & + Z_{w|w|}w|w| + Z_{q|q|}q|q| \\ & + (w - B_o)\cos\theta + u^2 Z_{uu}\delta_s, \end{aligned} \tag{1}$$

and its kinematic models in the vertical plane related to the inertial frame with the body frame are expressed as follows

$$\begin{cases} \dot{\theta} = q \\ \dot{z} = w\cos\theta - u\sin\theta \end{cases} \tag{2}$$

where w, q, z, and θ represent the heave velocity, the pith velocity, the depth variable, the pith angle, respectively; δ_s denotes the control fin angle; $[x_B, y_B, z_B]^{\mathrm{T}}$ is the vector representing the coordinates of the buoyancy center; $[x_G, y_G, z_G]^{\mathrm{T}}$ is the vector representing the coordinate of the center of gravity of the vehicle; I_{yy} denotes the moment of inertia of the vehicle about the pitch axis; u is the longitudinal velocity; $Z_{\dot{q}}, Z_{\dot{w}}, Z_{uq}, Z_{uw}, Z_{q|q|}, Z_{uu}, Z_{ww}, M_{\dot{q}}, M_{\dot{w}}, M_{w|w|}, M_{q|q|}, M_{uq}, M_{uu}, M_{uw}$ denote the hydrodynamics parameters; W and B_0 represent the weight and buoyancy of the underwater vehicle, respectively.

Given the state variable of $x = [w, q, \theta, z]^{\mathrm{T}}$, equation (2) can be simplified as the following compact form by ignoring the sufficiently small second-order viscous damping coefficient

$$\dot{x} = Ax + Bu + d \tag{3}$$

where d denotes the unmodeled dynamics and external interference and it is a matrix of four rows and one column; the matrix A is equal with $T^{-1}A'$, and the input matrix B is equal with $T^{-1}B'$, where the three vectors of T, A', and B' have the following forms: $T = \begin{bmatrix} m - Z_{\dot{w}} & -Z_{\dot{q}} & 0 & 0 \\ -M_{\dot{w}} & I_{yy} - M_{\dot{q}} & 0 & 0 \\ 0 & 0 & 1 & 0 \\ 0 & 0 & 0 & 1 \end{bmatrix}$, $A' = \begin{bmatrix} Z_{uw}u & Z_{uq} + mu & 0 & 0 \\ M_{uw}u & M_{uq}u & 0 & 0 \\ 0 & 1 & 0 & 0 \\ 1 & 0 & -u & 0 \end{bmatrix}$, $B' = \begin{bmatrix} Z_{uu}u^2 \\ M_{uu}u \\ 0 \\ 0 \end{bmatrix}$, in which the matrix T can be written as a block matrix: $T = \begin{bmatrix} R & 0 \\ 0 & I \end{bmatrix}$ and $R = \begin{bmatrix} m - Z_{\dot{w}} & -Z_{\dot{q}} \\ -M_{\dot{w}} & I_{yy} - M_{\dot{q}} \end{bmatrix}$. Thus, the inverse of matrix T is calculated as $T^{-1} = \begin{bmatrix} R^{-1} & 0 \\ 0 & I \end{bmatrix}$. The necessary and sufficient condition for matrix T invertible is that the matrix R is invertible. Substituting these parameters m, $Z_{\dot{w}}$, $Z_{\dot{q}}$, $M_{\dot{w}}$, and I_{yy} in the fourth section into matrix R yields that the matrix R is invertible. Therefore, the matrix T in this article is invertible.

When those unmodeled dynamics and external interference are neglected, the nominal dynamic model of equation (3) can be expressed as

$$\dot{x} = Ax + Bu \tag{4}$$

When the two uncertainties associated with system matrix and input matrix are considered in the kinematic model, the nonlinear dynamic model of equation (4) with uncertainty terms can be rewritten in the following form

$$\dot{x} = \Big(A + \Delta A\Big(a(t)\Big)\Big)x + \Big(B + \Delta B\Big(b(t)\Big)\Big)u + N \cdot n(t) \tag{5}$$

where $a(t)$ denotes an uncertainty vector associated with the system matrix; $b(t)$ represents an uncertainty vector associated with the input matrix; and $n(t)$ is an unmodeled dynamics and external interference, which is matched disturbance.

Orthogonal transformation of dynamic model

Equation (5) can be transformed into the block matrix form using the linear transformation

$$\hat{x} = Mx = [\hat{x}_1 \quad \hat{x}_2]^{\mathrm{T}} \tag{6}$$

where M denotes the transformation matrix. After transformation, equation (5) becomes

$$\begin{cases} \dot{\hat{x}}_1 = A_{11}\hat{x}_1 + A_{12}\hat{x}_2 + \Delta A_{11}\hat{x}_1 + \Delta A_{12}\hat{x}_2 + N_1 n(t) \\ \dot{\hat{x}}_2 = A_{21}\hat{x}_1 + A_{22}\hat{x}_2 + B_2 u + \Delta A_{21}\hat{x}_1 + \Delta A_{22}\hat{x}_2 \\ \qquad + \Delta B u + N_2 n(t) \end{cases} \tag{7}$$

where $M \cdot A \cdot M^{\mathrm{T}} = \begin{bmatrix} A_{11} & A_{12} \\ A_{21} & A_{22} \end{bmatrix}$, $M \cdot \Delta A \cdot M^{\mathrm{T}} = \begin{bmatrix} \Delta A_{11} & \Delta A_{12} \\ \Delta A_{21} & \Delta A_{22} \end{bmatrix}$, $M \cdot \Delta B = [0 \ \Delta B_2]^{\mathrm{T}}$, and $M \cdot N = [N_1 \ N_2]^{\mathrm{T}}$.

Assumption 1. These vectors of parameter uncertainty, input uncertainty, and interference uncertainty are bounded. The uncertainty parameters in equation (7) take the form of $\Delta A_{11} = A_{12}l_{11}$, $\Delta A_{12} = A_{12}D_1$, $N_1 = A_{12}E_1$, $2A_{21} = B_2 l_{21}$, $1A_{22} = B_2 l_{22}$, $\Delta B_2 = B_2 D_2$, and $N_2 = \mathrm{B}_2 E_2$. These bounded values of the matrix parameters are used to represent the uncertainty.

Substituting those uncertain parameters in Assumption 1 into equation (7) yields

$$\begin{cases} \dot{\hat{x}}_1 = A_{11}\hat{x}_1 + A_{12}[(I + D_1)\hat{x}_2 + h_1] \\ \dot{\hat{x}}_2 = A_{21}\hat{x}_1 + A_{22}\hat{x}_2 + B_2[(I + D_2)u + h_2] \end{cases} \tag{8}$$

where $\eta_1 = l_{11}\hat{x}_1 + E_1 n(t)$ and $\eta_2 = l_{21}\hat{x}_1 + l_{22}\hat{x}_2 + E_2 n(t)$ represent uncertainty term in the dynamic model, and their corresponding absolute values are bounded as follows: $||\eta_1|| \leq \max(||l_{11}|| \cdot ||\hat{x}_1||) + \max\left(||E_1 n(t)||\right)$, $||\eta_2|| \leq \max(||l_{21}|| \cdot ||\hat{x}_1||) + \max(||l_{22}|| \cdot ||\hat{x}_2||) + \max\left(||E_2 n(t)||\right)$. Matrices D_i ($i = 1, 2$) are assumed to satisfy the following inequality: $1 + \max\left\{\lambda_{\min}\left[\frac{D_i + D_i^{\mathrm{T}}}{2}\right]\right\} \geq \gamma_{D_i}$.

Controller design

Sliding mode controller

A variable structure robust controller is proposed to control the unmatched uncertainty linear system defined in equation (5). Let $s(t)$ be a sliding surface defined by equation $s(\hat{x}_1, \hat{x}_2) = 0$. Then, the sliding mode surface can be expressed as

$$s = C\hat{x} = C_1\hat{x}_1 + C_2\hat{x}_2 = 0 \tag{9}$$

where C_1 is calculated by equation $|\lambda I + (A_{11} - A_{12}C_1)| = 0$; C_2 is an identity matrix and $s(\hat{x}_1, \hat{x}_2) = 0$ is defined on the basis of the pole placement which places all poles of the closed system in a certain region in the left side of the complex plane to ensure the closed system stability.

Taking the time derivative of the sliding mode surface in equation (9) and then substituting equation (8) into the result of the time derivative of the sliding mode surface in equation (9) yield

$$\begin{aligned}\dot{s} = C_1\dot{\hat{x}}_1 + C_2\dot{\hat{x}}_2 = Ks + L\dot{\hat{x}}_1 + B_2[(I + D_2)u + \eta_2] \\ + C_1A_{12}[\eta_1 + D_1(s - C_1\hat{x}_1)]\end{aligned} \tag{10}$$

where $K = A_{22} + C_1A_{12}$, $L = A_{12} - A_{22}C_1 + C_1H$, $H = A_{11} - A_{12}C_1$.

The robust SMC is designed as the following combinational parts of the equivalent control law and continue robust control law

$$u = u_{\mathrm{cr}} + u_{\mathrm{eq}} \tag{11}$$

and the equivalent control law in the SMC is designed as

$$u_{\mathrm{eq}} = -B_2^{-1}[L\hat{x}_1 + (K - K*)s] \tag{12}$$

where $K*$ is located in the negative side of the half plane on the complex plane. Substituting equation (12) into equation (10) yields

$$\dot{s} = K * s + B_2[(I + D_2)u_{cr} + \eta_3] \tag{13}$$

where $\eta_3 = R_1 s + R_2 + R_3 n(t)$, $R_1 = l_{22} + B_2^{-1}C_1A_{12}D_1 - D_2B_2^{-1}(K - K*)$, $R_2 = l_{21} - l_{22}C_1 + B_2^{-1}C_1A_{12}l_{11} - B_2^{-1}C_1A_{12}C_1 - D_2B_2^{-1}L$, $R_3 = E_2 + B_2^{-1}C_1A_{12}E_1$.

A continue robust control law in the SMC is defined as

$$u_{cr} = -r_{D_2}^{-1}\left(1 + \frac{\rho}{||B_2^{\mathrm{T}}Ps|| + \sigma}\right)B_2^{\mathrm{T}}Ps \tag{14}$$

where $\rho \geq \bar{k}_1||x_1|| + \bar{k}_2$, $\bar{k}_1 = \max||R_2||$, $\bar{k}_2 = \max||R_3 n(t)||$, and σ is a positive constant; the vector P in equation (14) can be calculated by solving the following Riccati equation

$$K*^T P + PK* - PB_2B_2^{\mathrm{T}}P + Q = 0 \tag{15}$$

Theorem 1.[22] For system $\dot{x} = f(x, t)$, there is one mapping function V as $U \times J \rightarrow R$ satisfies the following conditions: there are some constants $\lambda > 0$ and a scalar function $\bar{\lambda}$ as $U \rightarrow R$ such that $\lambda||x(t)||^2 \leq ||V(t)|| \leq \bar{\lambda}(x)||x(t)||^2$ and $\dot{V}(x, t) \leq -\lambda_V\bar{\lambda}(\mathrm{t})||x(t)||^2 + \varepsilon$ for all $(x, t) \in U \times J$ and $x \in R^n$.

Then, the terminal value of the system is globally bounded as $t \rightarrow \infty$

$$||x(t)|| \leq \frac{1}{\lambda}V(x_0, t_0)e^{-\lambda_V(t - t_0)} + \frac{\varepsilon}{\lambda\lambda_V}\left(1 - e^{-\lambda_V(t - t_0)}\right) \leq \frac{\varepsilon}{\lambda\lambda_V} \tag{16}$$

where $\frac{\varepsilon}{\lambda\lambda_V}$ is a positive constant. The bounded terminal value system is essential condition for the asymptotical stability of the system.

Theorem 2. Given that the dynamic model defined in equation (5) satisfies Assumption 1, the sliding mode control laws in equations (12) and (14), and the Riccati-like equation in equation (15) guarantee the global stability of the closed-loop system.

Proof. Now, the following Lyapunov function is defined

$$V(t) = s^{\mathrm{T}}Ps \tag{17}$$

Taking the time derivative of $V(t)$, and substituting the equation (13) into the time derivative yields

$$\begin{aligned}\dot{V}(t) &= \dot{s}^{\mathrm{T}}Ps + s^{\mathrm{T}}P\dot{s} \\ &= s^{\mathrm{T}}PK^*s + s^{\mathrm{T}}K^{*\mathrm{T}}Ps + u_{\mathrm{cr}}^{\mathrm{T}}(I + D_2)^{\mathrm{T}}B_2^{\mathrm{T}}Ps \\ &\quad + s^{\mathrm{T}}PB_2(I + D_2)u_{\mathrm{cr}} + \eta_3^{\mathrm{T}}B_2^{\mathrm{T}}Ps + s^{\mathrm{T}}PB_2\eta_3\end{aligned} \tag{18}$$

Let $\dot{V}_1(t) = u_{\mathrm{cr}}^{\mathrm{T}}(I + D_2)^{\mathrm{T}}B_2^{\mathrm{T}}Ps + s^{\mathrm{T}}PB_2(I + D_2)u_{\mathrm{cr}}$ and $\dot{V}_2(t) = \eta_3^{\mathrm{T}}B_2^{\mathrm{T}}Ps + s^{\mathrm{T}}PB_2\eta_3$ and substituting the continuous robust control law in equation (14) into $\dot{V}_1(t)$ yields

$$\begin{aligned}\dot{V}_1(t) &= u_{\mathrm{cr}}^{\mathrm{T}}(I + D_2)^{\mathrm{T}}B_2^{\mathrm{T}}Ps + s^{\mathrm{T}}PB_2(I + D_2)u_{\mathrm{cr}} \\ &= -2r_{D_2}^{-1}\left[1 + \frac{\rho}{||B_2^{\mathrm{T}}Ps|| + \sigma}\right]s^{\mathrm{T}}PB_2\left(I + \frac{D_2 + D_2^{\mathrm{T}}}{2}\right)B_2^{\mathrm{T}}Ps\end{aligned} \tag{19}$$

By using *Assumption* 1, equation (19) becomes

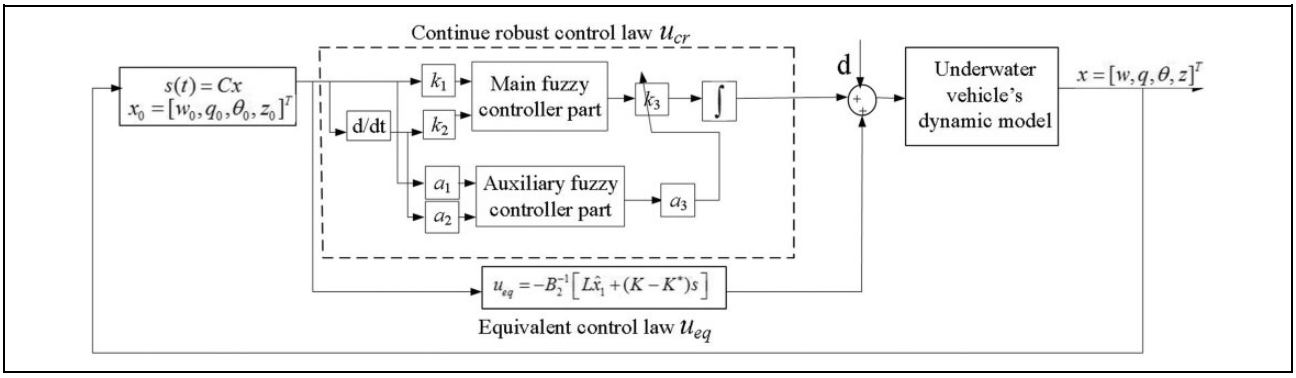

Figure 2. Block diagram of the AFSMC. AFSMC: adaptive fuzzy sliding mode controller.

$$\dot{V}_1(t) \le -2\left[1 + \frac{\rho}{||B_2^T Ps|| + \sigma}\right] s^{\mathrm{T}} P B_2 B_2^{\mathrm{T}} P s \tag{20}$$

Substituting the η_3 in equation (13) into $\dot{V}_2(\mathrm{t})$ yields

$$\begin{aligned}\dot{V}_2(t) &= \eta_3^{\mathrm{T}} B_2^{\mathrm{T}} P s + s^{\mathrm{T}} P B_2 \eta_3 \\ &= s^{\mathrm{T}} R_1^{\mathrm{T}} B_2^{\mathrm{T}} P s + s^{\mathrm{T}} P B_2 R_1 s + (R_2 x_1 + R_3 n)^{\mathrm{T}} B_2^{\mathrm{T}} P s \\ &\quad + s^{\mathrm{T}} P B_2 (R_2 x_1 + R_3 n)\end{aligned} \tag{21}$$

Since $(R_1 s)^{\mathrm{T}} B_2^T P s + (B_2^{\mathrm{T}} P s)^{\mathrm{T}} R_1 s \le (R_1 s)^T R_1 s + (B_2^T P s)^{\mathrm{T}} B_2^T P s$, equation (21) can be rewritten as follows

$$\begin{aligned}\dot{V}_2(t) &\le s^{\mathrm{T}} R_1^{\mathrm{T}} R_1 s + s^{\mathrm{T}} P B_2 B_2^{\mathrm{T}} P s + 2||R_2 x_1 + R_3 n||||B_2^{\mathrm{T}} P s|| \\ &\le s^{\mathrm{T}} R_1^{\mathrm{T}} R_1 s + s^{\mathrm{T}} P B_2 B_2^{\mathrm{T}} P s + 2\rho||B_2^{\mathrm{T}} P s||\end{aligned} \tag{22}$$

Substituting equations (20) and (22) into equation (18) results in

$$\begin{aligned}\dot{V} &\le s^{\mathrm{T}}(-P B_2 B_2^{\mathrm{T}} P + R_1^{\mathrm{T}} R_1 + K^{*\mathrm{T}} P + P K^*) s \\ &\quad - \frac{2\rho}{||B_2^{\mathrm{T}} P_2 s|| + \sigma} s^{\mathrm{T}} P B_2 B_2^{\mathrm{T}} s + 2\rho||B_2^{\mathrm{T}} P s||\end{aligned} \tag{23}$$

Substituting equation (15) into equation (23) yields

$$\dot{V} \le -s^{\mathrm{T}}(Q - R_1^{\mathrm{T}} R_1) s - \frac{2\rho}{||B_2^{\mathrm{T}} P s|| + \sigma}||B_2^{\mathrm{T}} P s||^2 + 2\rho||B_2^{\mathrm{T}} P s|| \tag{24}$$

Since $-\frac{||B_2^{\mathrm{T}} P s||^2}{||B_2^{\mathrm{T}} P s|| + \sigma} \le -||B_2^{\mathrm{T}} P s|| + \sigma, Q \ge R_1^{\mathrm{T}} R_1$, equation (24) can be rewritten as follows

$$\begin{aligned}\dot{V} &\le -s^{\mathrm{T}}(Q - R_1^{\mathrm{T}} R_1) s + 2\rho\sigma \\ &\le -\lambda_{\min}(Q - R_1^{\mathrm{T}} R_1)||s||^2 + 2\rho\sigma\end{aligned} \tag{25}$$

From the equation (25), the second property in Theorem 1 can then be obtained as $\dot{V}(x, t) \le -\lambda_V \bar{\lambda}(t)||x(t)||^2 + \varepsilon, \forall x \epsilon R^{\mathrm{n}}$, where $\lambda_V \bar{\lambda} = \lambda_{\min}(Q - R_1^{\mathrm{T}} R_1)$ and $\varepsilon = 2\rho\sigma$. Therefore, using Theorem 1, the robust SMC defined in equations (12) and (14) can guarantee the asymptotical convergence of the target depth.

Adaptive fuzzy sliding mode controller

To improve the control performances, an adaptive fuzzy algorithm is employed to reduce the chattering issues. Figure 2 illustrates the principle of adaptive SMC.

As shown in Figure 2, the AFSMC is composed of a continuous robust control law of u_{cr} and an equivalent control law of u_{eq}. The adaptive fuzzy controller consists of two components: a main fuzzy controller component and an auxiliary fuzzy controller component. The knowledge base for the main fuzzy controller component contains a collection of fuzzy *if–then* rules with the following form (R_j): If x_1 is as A_{1j} and x_2 is as A_{2j}, then y is as B_j ($j = 1, 2, \ldots 1\ n$), where x_i ($i = 1, 2$) are input parameters of the main fuzzy control component; y is the output parameter of the main fuzzy control component; fuzzy sets A_{ij} and B_j are associated with the membership functions $\mu_{Aij}(x_i)$ and $\mu_{Bj}(y)$, respectively, and n is the number of fuzzy rules. The input membership function is defined as the following triangular and trapezoidal hybrid function

$$\mu_{A_{ij}}(x_i) = \begin{cases} 0 & x_i < a_{ij} \text{ or } x_i > c_{ij} \\ \dfrac{x_i - a_{ij}}{b_{ij} - x_i} & a_{ij} \le x_i \le b_{ij} \text{ and } j \ne 1 \\ \dfrac{c_{ij} - x_i}{c_{ij} - b_{ij}} & b_{ij} < x_i \le c_{ij} \text{ and } j \ne n \\ 1 & a_{i1} \le x_i \le b_{i1} \text{ or } b_{in} < x_i \le c_{in} \end{cases} \tag{26}$$

where a_{ij}, b_{ij}, and c_{ij} are fuzzy segmentation points. The output membership function is defined as the triangular membership function. The output parameter value of the main fuzzy control component with a weighted-center defuzzifier and a singleton fuzzifier can be expressed as follows

$$y = \sum_{j=1}^{n} \phi_j(x) w_j \tag{27}$$

Table 1. Fuzzy control row set in the main fuzzy control component.

k_1 s(t) / $k_2\dot{s}(t)$	NB	NM	NS	ZE	PS	PM	PB
NB	PB	PB	PB	PB	PM	PS	ZE
NM	PB	PB	PB	PM	PS	ZE	NS
NS	PB	PB	PM	PS	ZE	NS	NM
ZE	PB	PM	PS	ZE	NS	NM	NB
PS	PM	PS	ZE	NS	NM	NB	NB
PM	PS	ZE	NS	NM	NB	NB	NB
PB	ZE	NS	NM	NB	NB	NB	NB

Table 2. Adaptive fuzzy control row set in the auxiliary fuzzy control component.

a_1 s(t) / $a_2\dot{s}(t)$	NE	ZE	PE
NB	PB	PB	PB
NM	PB	PB	PB
NS	PB	PB	PM

where $\phi_j(x) = \mu_{A_{1j}}(x_1)\mu_{A_{2j}}(x_2)$ and w_j is the critical parameter value at the maximum of the output membership function μ_{B_j}. Equation (27) can be rearranged as

$$y = W_1^{\mathrm{T}}\Phi_1(x) \tag{28}$$

where $W_1^{\mathrm{T}} = [w_1, \cdots, w_n]$ and the vector of the fuzzy basis function is $\Phi_1^{\mathrm{T}}(x) = [\phi_1(x), \ldots, \phi_{\mathrm{n}}(x)]$.

The two input parameters of x_1 and x_2 in the main fuzzy control component are $k_1 s(t)$ and $k_2\dot{s}(t)$, respectively, and the output parameter of y is $\dot{u}_{\mathrm{cr}}/k_3$. The fuzzy rules of the main fuzzy controller component are summarized in Table 1. The output parameter $\dot{u}_{\mathrm{cr}}/k_3$ is equal to $W_1^{\mathrm{T}}\Phi_1\left(k_1 s(t), k_2\dot{s}(t)\right)$. To improve the consistency of a fuzzy system under the interference of unknown dynamic parameters or bounded external disturbances, the fuzzy system should contain a strong self-adaptive ability. A scale coefficient k_3 is selected as a freely adjustable parameter, and the auxiliary fuzzy control component is adopted to adjust scale coefficient k_3. Two input parameters in the auxiliary control component are denoted as $a_1 s(t)$ and $a_2\dot{s}(t)$, and its output parameter is defined as a_3. Through the main and auxiliary fuzzy control component, the existence and elimination of chattering can be demonstrated for SMC using a proposed Mamdani-type fuzzy inference system. The output of adaptive fuzzy controller is determined by the normalized values of $s(t)$ and $\dot{s}(t)$. The fuzzy control rules can be represented as the mapping of the input linguistic variables $s(t)$ and $\dot{s}(t)$ to the output linguistic variable u_{cr}. Through online learning, it can establish and regulate the fuzzy rules continuously for responding to the system's parameters and external disturbances. The fuzzy membership function and the defuzzifier of the auxiliary fuzzy control component are the same as those in the main fuzzy control component. Thus, the output parameter a_3 can be calculated as $a_3 = W_2^{\mathrm{T}}\Phi_1(a_1 s(t),\ a_2\dot{s}(t))$. The fuzzy rules in the auxiliary fuzzy control component are illustrated in Table 2. Replacing scale coefficient k_3 by the output parameter in the auxiliary fuzzy control component and integrating $\dot{u}_{\mathrm{cr}}$ would result in

$$u_{\mathrm{cr}} = \int W_1^{\mathrm{T}}\Phi_1\left(k_1 s(t), k_2\dot{s}(t)\right) W_2^{\mathrm{T}}\Phi_2\left(a_1 s(t), a_2\dot{s}(t)\right)\mathrm{d}t \tag{29}$$

The membership functions input parameters and output parameters of the adaptive fuzzy control are shown in Figures 3 and 4.

Simulation results and discussions

A 3-DOF REMUS underactuated underwater vehicle is taken as an example to examine the depth control ability of the above proposed AFSMC. The objective of the simulations is to examine the ability of the proposed controller in the depth control by forcing the proposed controller to track a desired depth at $z_{\mathrm{r}} = 0$ m. The weight of the underwater vehicle is calculated as $W = mg = 299$ N with $m = 30.48$ kg, $g = 9.81$ m/s^2, and its buoyancy force $B_0 = 306$ N. The center of gravity is defined as $[x_G, y_G, z_G]^{\mathrm{T}} = [0\text{ m}, 0\text{ m}, 0\text{ m}]^{\mathrm{T}}$, and the center of buoyancy is defined as $[x_B, y_B, z_B]^{\mathrm{T}} = [0\text{ m}, 0\text{ m}, 0\text{ m}]^{\mathrm{T}}$, the inertia moment of the vehicle about the pitch axis $I_{yy} = 3.45\ \mathrm{kg}\cdot\mathrm{m}^2$. The hydrodynamic coefficients were calculated using *Fluent* software (Fluent 14.0) by simulating both steady state and unsteady state. The obtained coefficients are listed as follows: $M_q = -4.88$ kg·m^2/rad, $M_{\dot{w}} = -1.93\ \mathrm{kg}\cdot\mathrm{m}$, $M_{w|w|} = 3.18$ kg, $M_{q|q|} = -188$ kg·m^2/rad, $M_{uu\delta} = -6.15$ kg/rad, $M_{uq} = -2$ kg·m/rad, $M_{uw} = 24$ kg, $Z_{\dot{w}} = -35.5$ kg, $Z_{\dot{q}} = -1.93\ \mathrm{kg}\cdot\mathrm{m}/\mathrm{rad}$, $Z_{ww} = -131$ kg/m, $Z_{q|q|} = -0.632$ kg·m/rad^2, $Z_{uw} = -28.6$ kg/m, $Z_{uq} = -5.22$ kg/rad, and $Z_{uu\delta} = -6.15$ kg/(m·rad).

The start and desired depths in the simulation case are given as $z_0 = 2$ m and $z_r = 0$ m, respectively. The initial states set as $w_0 = 0.02$ m/s, $q_0 = 0.04$ rad/s, $\theta_0 = 0.1$ rad, $z_0 = 2$ m. These uncertainty parameters in equation (7) take the following values: $\Delta A = \begin{bmatrix} 0 & 0 & 0 & 0.1 \\ 0 & 0 & 0 & 0.01 \\ 0 & 0 & 0 & 0.769 \\ 0.1\times\sin t & 0 & 0 & 0 \end{bmatrix}$, $\Delta B = 0$, $N = \begin{bmatrix} -0.0722 \\ -0.722 \\ 0 \\ 0 \end{bmatrix}$, $n(t) = 2$. The two matrices of the sliding mode surface in equation (9) are defined as $C_1 = [\,1.02 \quad -1 \quad -1.46\,]^{\mathrm{T}}$ and $C_2 = 1$. The constants

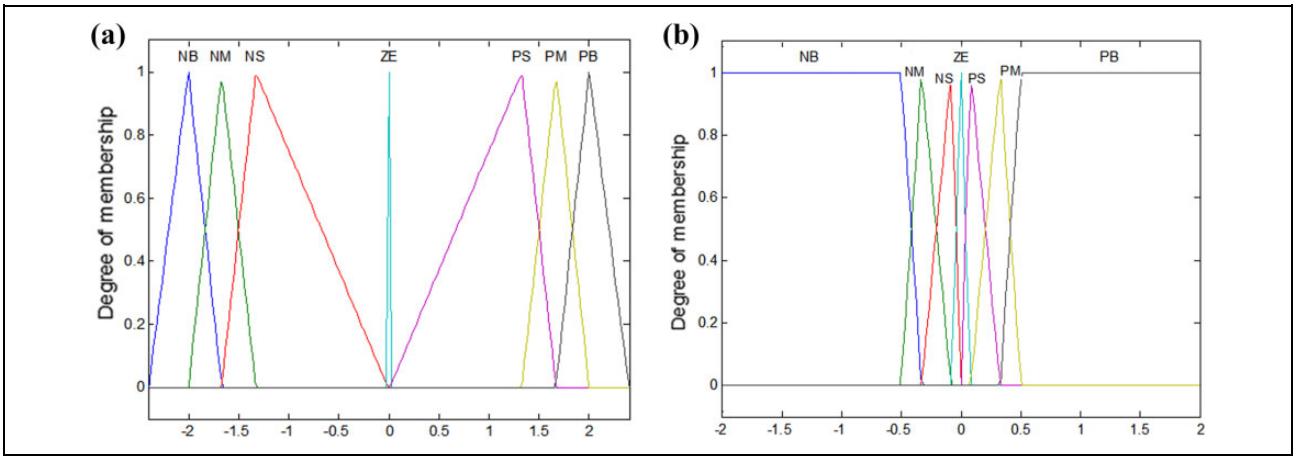

Figure 3. Membership functions of fuzzy input and output parameters in the main fuzzy control law: (a) the input variable s and $\dot{s}$; (b) the output variable $\dot{u}_{cr}/k_3$.

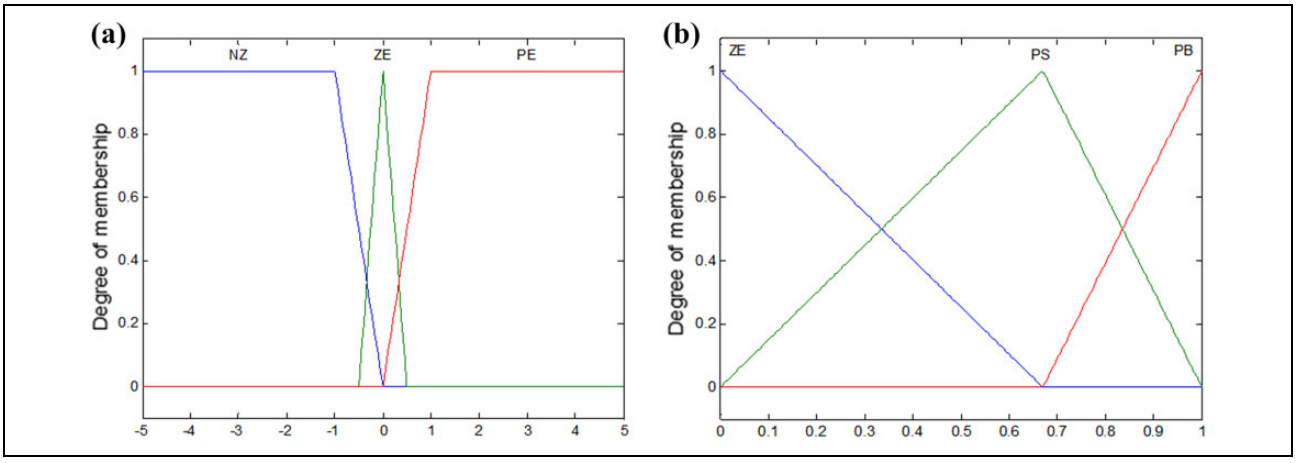

Figure 4. Membership functions in the auxiliary control law: (a) the input variables s and $\dot{s}$; (b) the output variable a_3.

σ, r_{D1}, and r_{D2} in equation (14) are selected as $\sigma = 1.5$, $r_{D1} = 1.5$ and $r_{D2} = 0.8$. The two parameters Q and $K*$ in the Riccati equation (15) are chosen as 2.3 and -1, respectively.

Case 1. The SMC in equation (11) is applied in the nominal system and uncertain model for the 3-DOF REMUS AUV. Its control law is defined as follows

$$u = u_{cr} + u_{eq} = -r_{D_2}^{-1}\left(1 + \frac{\rho}{||B_2^{\mathrm{T}}Ps|| + \sigma}\right)B_2^{\mathrm{T}}Ps - B_2^{-1}[L\hat{x}_1 + (K - K*)s] \tag{30}$$

Under the control action of SMC, the depth control performance of the SMC is illustrated in Figure 5. It can be observed from Figure 5 that the SMC performs much better and more satisfactory in the nominal system than in uncertain model. As observed from Figure 5, it takes about 15 s from the initial state to the desired depth position. However, a large steady-state error exists for the control of systems with parameter uncertainties and external disturbances. Therefore, some additional appropriate compensation control schemes and chattering elimination method need to be developed and incorporated in the SMC to minimize the impact of uncertainties on the depth control performances.

Case 2. An AFSMC is designed to minimize the impact of uncertainties on the depth control performances for the 3-DOF REMUS AUV. Its control law is expressed as follows

$$u = u_{cr} + u_{eq} = \int W_1^{\mathrm{T}}\Phi_1\left(k_1 s(t), k_2\dot{s}(t)\right)W_2^{\mathrm{T}}\Phi_2\left(a_1 s(t), a_2\dot{s}(t)\right)\mathrm{d}t - B_2^{-1}[L\hat{x}_1 + (K - K*)s] \tag{31}$$

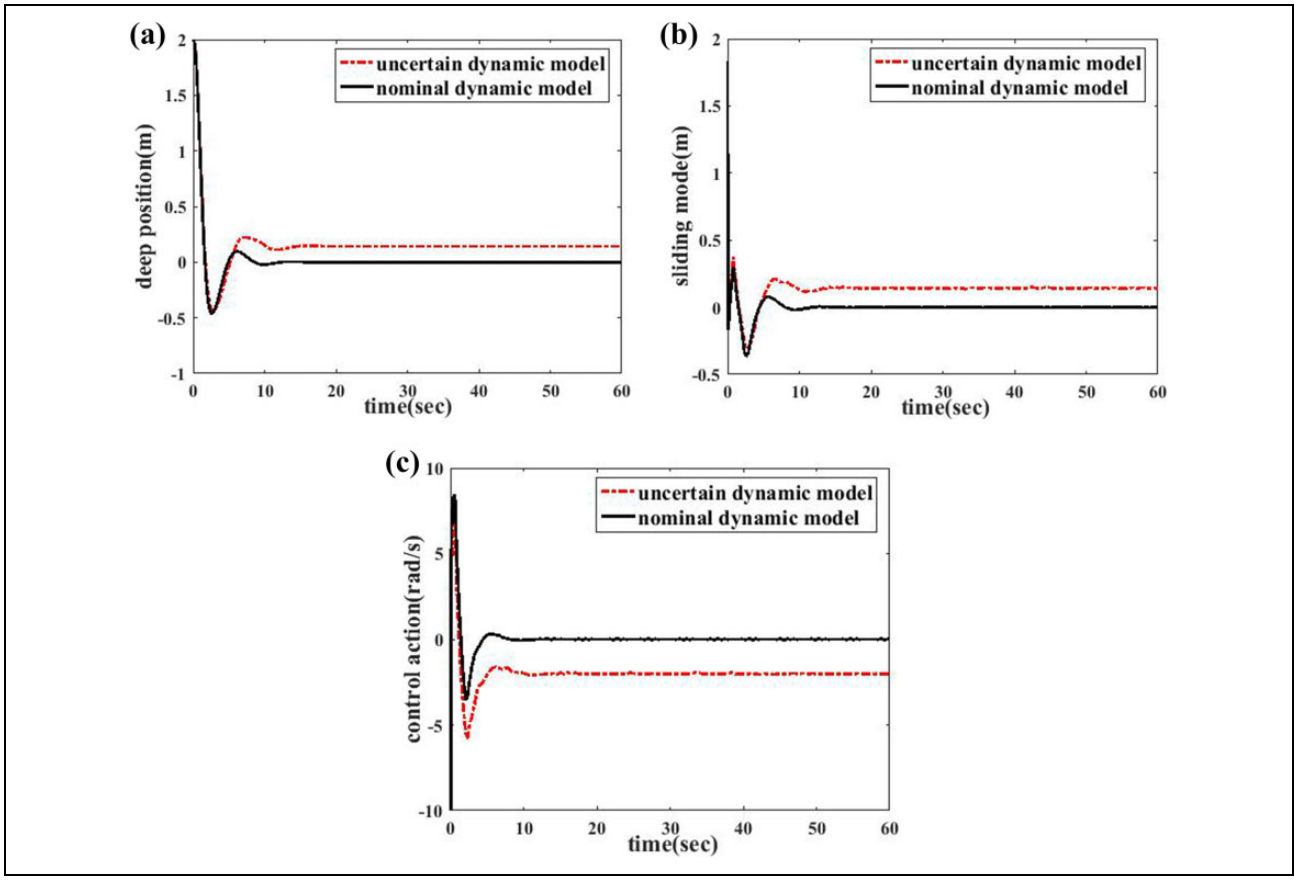

Figure 5. Depth control performances when the SMC is applied in the nominal system and uncertainty dynamic model: (a) depth position; (b) sliding mode surface; (c) control action. SMC: sliding mode controller.

In the main fuzzy controller component, the triangular membership functions with the central values $\{-2; -0.5; -0.33; -0.08; 0; 0.08; 0.33; 0.5; 2\}$ are adopted for the two input parameters $k_1 s(t)$ and $k_2 \dot{s}(t)$. The triangular membership function with the central value $\{-2.4; -2; -1.67; -1.33; -0.01; 0; 0.01; 1.33; 1.67; 2; 2.4\}$ is also adopted for the output parameter $\dot{u}_{cr}/k_3$. At the same time, the triangular membership functions with the central values $\{-5; -1; -0.5; 0; 0.5; 1; 5\}$ applied into the auxiliary fuzzy controller component. With selected constants $k_1 = 1.5$, $k_2 = 1$, $k_3 = 30$, $a_1 = 1$, $a_2 = 2$, the depth control performances of the adaptive fuzzy sliding mode control law in equation (31) for the 3-DOF REMUS AUV with uncertain dynamic model are illustrated in Figure 6. It can be observed from Figure 6 that the proposed AFSMC performs extremely well in overshoots elimination and also converges very fast even with the external disturbance and parameter uncertainties.

Some comparative studies were also conducted between the SMC and the proposed AFSMC. The desired trajectories tracked by the two control algorithms are the same as those in the mentioned simulation cases. For the convenience of comparisons, the depth, the control action, and sliding mode surface tracking errors in those cases are calculated by the following tracking error equations over one training cycle of a trajectory

$$E_z = \frac{1}{N}\sum_{i=1}^{N} \left|\left|z_d - z_i\right|\right|^2 (\mathrm{m})^2,$$
$$E_u = \frac{1}{N}\sum_{i=1}^{N} \left|\left|u_d - u_i\right|\right|^2 (\mathrm{rad/s})^2,$$
$$E_s = \frac{1}{N}\sum_{i=1}^{N} \left|\left|s_d - s_i\right|\right|^2 (\mathrm{m})^2 \qquad (32)$$

where E_z, E_u, and E_s represent the depth tracking error, the control action error, and the sliding mode surface error, respectively; N denotes the element number of the depth vector; z_d, u_d, s_d are the desired trajectories and z_i, u_i, s_i are the actual trajectories. The tracking errors of those cases after the convergence are summarized in Table 3. It is clearly demonstrated from Table 3 that the AFSMC scheme in case 2 has a superior performance in tracking errors minimization over the SMC scheme in case 1.

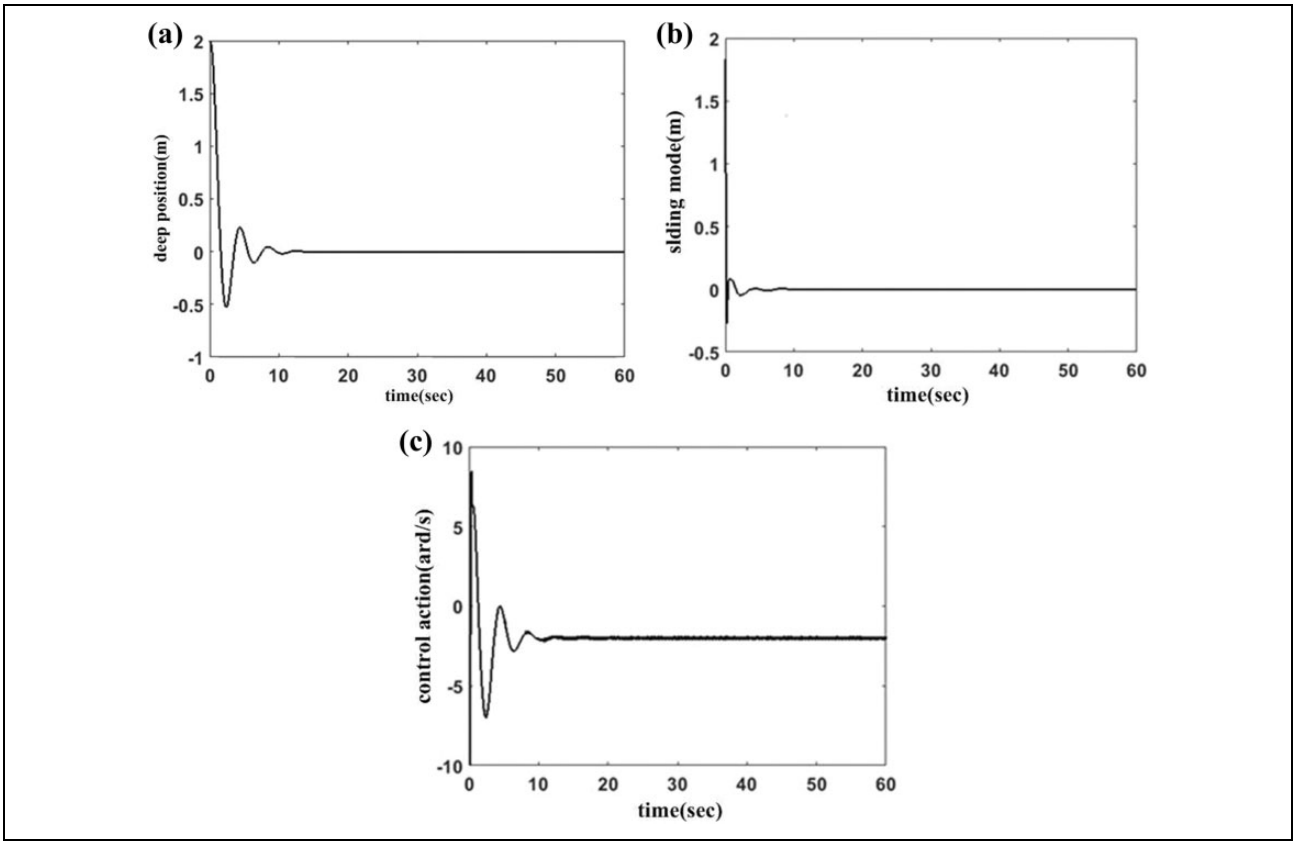

Figure 6. Depth control performances for AFSMC: (a) depth position; (b) sliding mode surface; (c) control action. AFSMC: adaptive fuzzy sliding mode controller.

Table 3. Tracking errors in three cases.

	Errors		
Control schemes	E_z (m)^2	E_u (rad/m)^2	E_s (m)^2
Case 1 (SMC)	0.0201	0.0010	0.0203
Case 2 (AFSMC)	7.9704e−06	2.0950e−04	1.7104e−05

SMC: sliding mode controller; AFSMC: adaptive fuzzy sliding mode controller.

Conclusions

In this article, an AFSMC was proposed to deal with the depth control of an underactuated underwater vehicle based on the state-dependent Riccati equation. An adaptive fuzzy control algorithm is embedded into the SMC to reduce the static error in the transient and steady states in the existence of unknown system parameters and external disturbances. The adaptive fuzzy control algorithm is composed of a main fuzzy controller component and an auxiliary fuzzy controller component, where an auxiliary fuzzy control unit is designed to automatically adjust the scale factor of the main fuzzy controller output. Moreover, the stability and convergence properties of the closed-loop system are demonstrated using Lyapunov stability theory and final value bounded theorem. Numerical simulation results have clearly demonstrated that the proposed AFSMC is superior over the SMC in improving the dynamic and static performances of the entire control system including the errors reduction, rapid convergence, and chattering elimination.

Declaration of conflicting interests

The author(s) declared no potential conflicts of interest with respect to the research, authorship, and/or publication of this article.

Funding

The author(s) disclosed receipt of following financial support for the research, authorship, and/or publication of this article: This work was financially supported by the Major Scientific and Technological Innovation Project of Shandong Province with Grant No. 2017CXGC0923 and Key Research and Development Program of Shandong Province Grant Nos. 2017GGX30112 and 2018GGX103025.

ORCID iD

Yuan Chen https://orcid.org/0000-0002-9358-7298

References

1. Yuh J. Learning control for underwater robotic vehicles. *IEEE Control Syst Mag* 1994; 14(2): 39–46.

2. Goheen K and Jeffreys E. Multivariable self-tuning autopilots for autonomous and remotely operated underwater vehicles. *IEEE J Oceanic Eng* 1990; 15(3): 144–151.
3. Lakhekar G and Waghmare L. Robust maneuvering of autonomous underwater vehicle: an adaptive fuzzy PI sliding mode control. *Intel Serv Robot* 2017; 10(3): 195–212.
4. Ma Z, Feng J, and Yang J. Research on vertical air-water transmedia control of Hybrid Unmanned Aerial Underwater Vehicles based on adaptive sliding mode dynamical surface control. *Int J Adv Robot Syst* 2018; 15(2): 1–10. DOI: 10.1177/1729881418770531.
5. Sarfraz M, Rehman F, and Shah I. Robust stabilizing control of nonholonomic systems with uncertainties via adaptive integral sliding mode: an underwater vehicle example. *Int J Adv Robot Syst* 2017; 14(5): 1–11. DOI: 10.1177/1729881417732693.
6. Zhang W, Liang Z, and Sun X. Path following control for an under-actuated UUV based on adaptive sliding mode control. *Int J Robot Autom* 2017; 32(5): 458–470.
7. Bessa W, Dutra M, and Kreuzer E. An adaptive fuzzy sliding mode controller for remotely operated underwater vehicles. *Robot Auton Syst* 2010; 58(1): 16–26.
8. Yang J and Kim J. Sliding mode control for trajectory tracking of nonholonomic wheeled mobile robots. *IEEE Trans Robot Autom* 1999; 15(3): 578–587.
9. Savkin A and Wang C. A simple biologically inspired algorithm for collision-free navigation of a unicycle-like robot in dynamic environments with moving obstacles. *Robotica* 2013; 31(6): 993–1001.
10. Chen Y, Wang K, Zhai L, et al. Feedforward fuzzy trajectory compensator with robust adaptive observer at input trajectory level for uncertain multi-link robot manipulators. *J Franklin Inst* 2017; 354(8): 3237–3266.
11. Valilou S and Khosrowjerdi M. Robust sliding mode control design for mismatched uncertain systems with a GH2/H_∞ performance. *Asian J Control* 2015; 17(5): 1848–1856.
12. Chatchanayuenyong T and Parnichkun M. Neural network based-time optimal sliding mode control for an autonomous underwater robot. *Mechatronics* 2006; 16(8): 471–478.
13. Wang Y, Gu L, and Gao M. Multivariable output feedback adaptive terminal sliding mode control for underwater vehicles. *Asian J Control* 2016; 18(1): 247–265.
14. Ouyang P, Acob J, and Pano V. PD with sliding control for trajectory tracking of robotic system. *Robot Comput Integr Manuf* 2014; 30(2): 189–200.
15. Chen Z and Zhang J. Adaptive fuzzy sliding mode control for uncertain nonlinear system. In: *International conference on machine learning & cybemetics*, Xi'an China, 2 November – 5 November 2003, paper no. v2, pp. 1044–1047. New York: IEEE.
16. Aloui S, Pagès O, and Hajjaji A. Robust Adaptive fuzzy sliding mode control design for a class of MIMO underactuated system. In: *IFAC proceedings volumes*, Milan Italy, 28 August – 2 September 2011, paper no. v 18, PART 1, pp. 11127–11132. Laxenburg: IFAC Secretariat.
17. Lakhekar G and Saundarmal V. Novel adaptive fuzzy sliding mode controller for depth control of an underwater vehicles. In: *International conference on fuzzy systems*, Hyderabad India, 7 July – 10 July. 2013, paper no. 6622573. New York: IEEE.
18. Lakhekar G and Saundarmal V. Robust self tuning of fuzzy sliding mode control. In: *International conference on computing, communications and networking technologies*, Tiruchengode India, 4–6 July, 2013, paper no. 6726610. Washington: IEEE Computer Society Washington.
19. Amer A, Sallam E, and Elawady W. Quasi sliding mode-based single input fuzzy self-tuning decoupled fuzzy PI control for robot manipulators with uncertainty. *Robust Nonlin Control* 2012; 22(18): 2026–2054.
20. Esfahani H, Azimirad V, and Danesh M. A time delay controller included terminal sliding mode and fuzzy gain tuning for underwater vehicle-manipulator systems. *Ocean Eng* 2015; 107: 97–107.
21. Naik M and Singh S. State-dependent Riccati equation-based robust dive plane control of AUV with control constraints. *Ocean Eng* 2001; 34(11–12): 1711–1723.
22. Mei S, Shen T, and Liu K. *Modern robust control theory and application*. Bejing: Tsinghua University Press, 2002, p. 120.